

Early Emphysema in the Tight Skin and Pallid Mice

Roles of Microfibril-Associated Glycoproteins, Collagen, and Mechanical Forces

Satoru Ito, Erzsébet Bartolák-Suki, J. Michael Shipley, Harikrishnan Parameswaran, Arnab Majumdar, and Bélâ Suki

Department of Biomedical Engineering, Boston University, Boston; Aeris Therapeutics, Inc., Woburn, Massachusetts; and Washington University School of Medicine, St. Louis, Missouri

The nature of the development of emphysema in the tight skin (Tsk) and the pallid (Pa) mice are not well understood. We assessed the mechanical and nonlinear properties of the respiratory system, the alveolar structure, and the levels of microfibril-associated glycoproteins (MAGP) 1 and 2 in Tsk mice with developmental emphysema; in Pa mice, which are thought to develop adult onset emphysema; and their background, the C57BL/6 mice, at an age of 7 wk. Minor differences between collagen-related elastic properties of the lungs of the Pa and C57BL/6 mice were seen at this early age. The lungs of the Tsk mice were significantly softer yet more nonlinear than those of the Pa and C57BL/6 mice. The MAGP-1 levels were similar in all three groups. However, the level of MAGP-2, which is associated with both fibrillin-1 and collagen, was higher in the Tsk than in the Pa mice, which also had more MAGP-2 than the C57BL/6. Both the mean and the variance of alveolar diameters were larger in the Tsk than in the other two groups, while the variance in the Pa was larger than in the C57BL/6 mice, implying early development of heterogeneity. Using a network model of the parenchyma, we linked the pathophysiologic changes in the Tsk mice to mechanical forces and failure of the alveolar walls. Our findings suggest the possibility that MAGP-2-related abnormal collagen assembly, combined with mechanical forces, is involved in the progression of emphysema in the Tsk mice.

Keywords: alveoli; destruction; elastance; progression; resistance

The tight skin (Tsk) mice spontaneously develop pulmonary emphysema and skin fibrosis early in life. A duplication of the fibrillin-1 gene results in a larger than normal fibrillin-1 (1, 2), a glycoprotein, which aids the deposition of extracellular matrix (ECM) components during development and remodeling (1, 3). The homozygous Tsk mice die *in utero*, but the heterozygous mice live a normal life span despite various organ disorders (4–6).

Crossing Tsk/+ and interleukin (IL)-4+/- mice disrupts one or both IL-4 alleles with ~ 30% survival rate (7). Although these mice do not have cutaneous hyperplasia, they still develop emphysema. Furthermore, while the elimination of the receptor IL-4R α or the deletion of one allele of transforming growth factor (TGF)- β results in diminished dermal thickening, these mice also develop emphysema (8). Since IL-4 regulates TGF- β (7), the cytokines that cause skin fibrosis in these mice are not responsible for the pathogenesis of emphysema.

What causes emphysema in these mice? Several mechanisms, including protease-antiprotease imbalance (9), inflammation

(10, 11), abnormal ECM remodeling (12), and mechanical forces (13), have been proposed to be involved in the development of emphysema. However, the pathogenesis, persistence, and progression of emphysema are not understood (14, 15).

Previously, we found that mechanical forces can rupture the alveolar walls from elastase-treated rats (16). Subsequently, we argued that abnormal collagen stiffness is likely involved in the progression of emphysema (13). The collagen in the alveoli protects the tissue from rupture in the normal lung. Hence, the alveoli may not be destroyed unless the collagen network is destabilized. Accordingly, we hypothesized that the strength of collagen in the Tsk alveoli is compromised due to abnormal ECM assembly related to the Tsk fibrillin-1. Consequently, transpulmonary pressure and stresses from the superimposed breathing generate sufficient forces that are able to rupture the alveolar walls, which leads to changes in structure and function characteristic of emphysema.

To test this hypothesis, we assessed the detailed mechanical and structural properties of the lungs from Tsk mice and compared them to those of the pallid (Pa) and their common background, the C57BL/6 mice. The Pa mouse has been reported to develop emphysema only around 10 mo of age, and it is related to a reduced serum α_1 -antitrypsin concentration (17) and is considered as the control of Tsk mice (4, 5, 18). To investigate the relation between fibrillin-1 and collagen assembly, we also examined the expression of a particular class of molecules, the microfibril-associated glycoproteins (MAGP) that have a direct association with both fibrillin and collagen (18, 19). Our results suggest a novel link among MAGP, collagen, and the nonlinear mechanical properties of the lung that we support using a network model of the parenchyma.

MATERIALS AND METHODS

See the online supplement for a more detailed description of the methods.

Animals

Heterozygous male tight skin (Tsk/+), homozygous Pallid (Pa+/Pa+) and C57BL/6 mice, of 7 wk of age were studied (Jackson Lab, Bar Harbor, ME). All animal procedures were approved by the Animal Care and Use Committees of Boston University.

Respiratory Mechanics

The C57BL/6 ($n = 8$), the Pa ($n = 8$), and the Tsk ($n = 8$) mice were anesthetized (IP 70 mg/kg), tracheostomized, cannulated, and mechanically ventilated (Flexivent; SCIREQ, Montreal, PQ, Canada) in supine position (tidal volume: 8 ml/kg; rate: 240 breaths/min). The quasi-static pressure–volume (P–V) curves were obtained during slow inflation (0.1 ml/s) from end-expiratory lung volume. Respiratory mechanics were assessed at four positive end-expiratory pressures (PEEPs) (0, 3, 6, and 9 cm H₂O) by measuring impedance data using forced oscillations. The impedance spectra were fit with a distributed model (20). Each pathway consisted of an airway resistance (Raw), tissue damping (G), and tissue elastance (H) (21), which was distributed hyperbolically between a minimum (Hmin) and a maximum (Hmax), whereas the hysteresivity (22) calculated as $\eta = G/H$ was kept constant.

(Received in original form and final form November 10, 2005)

This study was funded by NIH HL 59215.

Correspondence and requests for reprints should be addressed to Bela Suki, Ph.D., Dept. Biomedical Engin., Boston University, 44 Cummington Street, Boston, MA 02215. E-mail: bsuki@bu.edu

This article has an online supplement, which is accessible from this issue's table of contents at www.atsjournals.org

Am J Respir Cell Mol Biol Vol 34, pp 688–694, 2006

Originally Published in Press as DOI: 10.1165/rcmb.2006-0002OC on January 26, 2006

Internet address: www.atsjournals.org

The parameters R_{aw} , η , H_{min} , and H_{max} were estimated from the fits.

Dynamic nonlinearity was assessed by calculating the harmonic distortion index (K_d) using Fourier analysis (23, 24). The K_d in a linear system is zero. In a nonlinear system, the K_d measures the distortion and crosstalk due to dynamic system nonlinearities.

Histology and Morphometry

After the lungs were infused with 1% agarose solution (Sigma, St. Louis, MO) at 55°C to a transpulmonary pressure of 25 cm H₂O, thin tissue slices were prepared as previously (16). The alveolar walls were detected from autofluorescent images using an automated software and the mean and SD of diameters were calculated. Whole lung lavage samples (1 ml of saline) administered twice via the cannula were collected (five lungs per group). Total cells counts and differential cell analysis after rapid Wright's stain were performed under a light microscope.

Immunoblots

The Western blots were performed on tissues ($n = 4$ per group) using polyclonal anti-MAGP-1 (1:1,000; Elastin Products, Owensville, MO), and anti-MAGP-2 (1:1,000, from Dr. Shipley's laboratory) antibodies. Samples were fractionated (fractionPREP Fractionation System; BioVision, Mountain View, CA) and the cytosolic/extracellular fraction was used for further analysis. The samples were normalized to equal volume and separated by reducing SDS-polyacrylamide gel electrophoresis using 4–20% gradient gels, then blotted onto PVDF membrane (Bio-Rad, Hercules, CA). Western blots were performed using immunoblotting detected by chemiluminescence and quantified by densitometry.

Network Modeling

The parenchyma was modeled as a hexagonal network of springs with fixed boundaries. The springs force–displacement ($F-x$) relation was given by a third order polynomial: $F = a_1x + a_2x^2 + a_3x^3$. The spring properties were randomized, 1% of the springs was eliminated, and the equilibrium configuration was found by minimizing the elastic energy of the network (25). The network was stretched equibiaxially to several static strains mimicking PEEP. The network configuration was found along a single cycle of biaxial sinusoidal of 7% strain amplitude superimposed on static strains, and the stress was calculated from the total energy. Using Fourier analysis, the stiffness (Y) and K_d were calculated similarly as from the experimental data.

Statistical Analysis

Student's t test, F-test, and repeated-measure one-way or two-way ANOVA were used to evaluate statistical differences.

RESULTS

Quasi-Static Mechanical Properties

Figure 1 compares the quasi-static P–V curves obtained during volume-controlled inflation from end-expiratory lung volume. The airway pressure was significantly lower in the Tsk mice than in the Pa and the C57BL/6 mice ($P < 0.001$), but there was no difference between the latter two. The average quasi-static

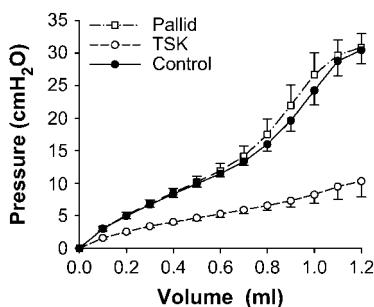


Figure 1. Quasi-static inspiratory pressure-volume relationships from end-expiratory lung volume of the C57BL/6, the Pa and the Tsk mice. Values are means \pm SD.

elastance of the respiratory system (the slope of the P–V curve between 0 and 1.15 ml) was significantly lower in the Tsk mice (9.0 ± 2.0 cm H₂O/ml) than in the Pa (26.9 ± 1.7 cm H₂O/ml) and the C57BL/6 (26.5 ± 1.7 cm H₂O/ml) mice ($P < 0.001$).

Dynamic Mechanical Properties

The mechanical parameters extracted from the distributed elastance model are shown as a function of PEEP in Figure 2. The airway resistance R_{aw} was PEEP dependent ($P < 0.001$) and lower in the TSK mice at all PEEPs ($P < 0.001$) than in the C57BL/6, which was not different from that in the Pa mice

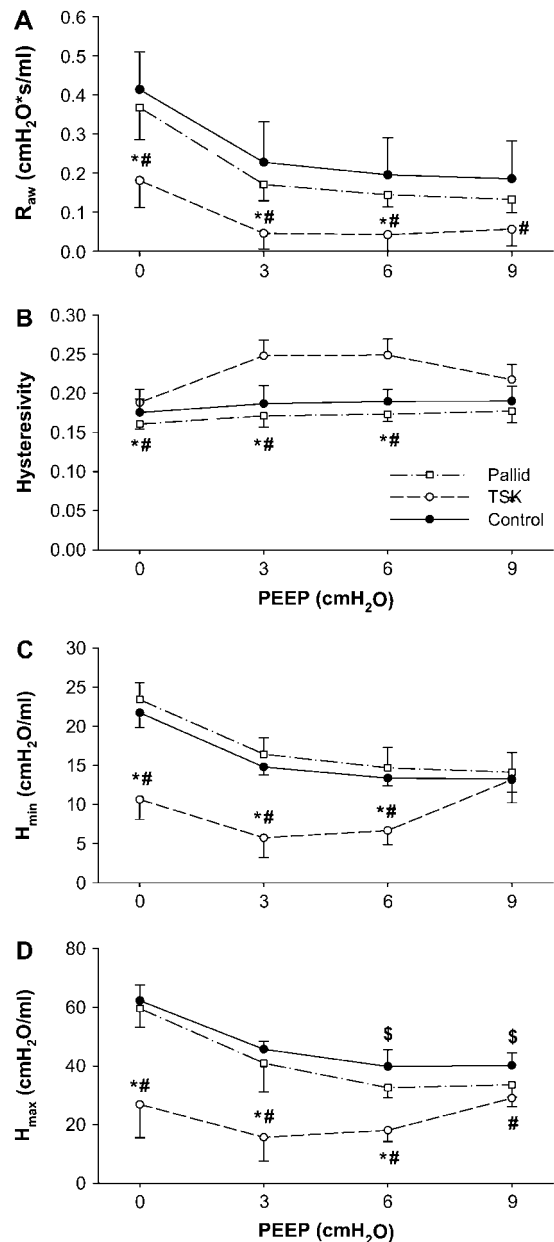


Figure 2. Parameters of respiratory mechanical properties obtained by fitting an impedance model to the data. Means \pm SD of airway resistance (R_{aw} , A), hysteresivity (B), minimum tissue elastance (H_{min} , C) and maximum tissue elastance (H_{max} , D) in the Tsk, Pa, and C57BL/6 mice as a function of PEEP. Statistical significance ($P < 0.05$) is denoted by * between Tsk and Pa, # between Tsk and C57BL/6, and \$ between Pa and C57BL/6.

(Figure 2A). Hysteresivity describing the relative energy dissipation per cycle in the tissue was PEEP-dependent in all three groups ($P < 0.01$), and was higher in the TSK mice (Figure 2B; $P < 0.001$). The elastic properties can be characterized by the minimum value (Hmin) and the maximum value (Hmax) of the tissue elastance of the respiratory system, which may be related to the physiologic function of emphysematous lesions and collagen in the lung, respectively (20). For the C57BL/6 and the Pa mice, both Hmin and Hmax decreased with increasing PEEP ($P < 0.001$) (Figures 2C and 2D). Interestingly, however, the Hmin and Hmax versus PEEP curves had a minimum at the 3 cm H₂O PEEP in the Tsk group, and increased with PEEP above 3 cm H₂O. The only parameter that was different between the C57BL/6 and the Pa groups was Hmax at the higher PEEP levels ($P < 0.02$).

Dynamic Nonlinearities

The harmonic distortion index K_d describes the dynamic nonlinear properties of the lung. When the lung is exposed to sinusoidal volume oscillations, the numerical value of K_d is associated with the extent to which the shape of the pressure–volume loop deviates from a pure ellipse—that is, it becomes “banana-like.” The K_d was significantly larger in the Tsk mice than in the C57BL/6 or Pa mice ($P < 0.001$). The K_d in the latter two groups were not different and hence the data from these groups were combined. Figure 3A shows the relation between the mean value of H (calculated from Hmin and Hmax) and K_d including data from all PEEP levels. There was strong linear relation between H and K_d both in the Tsk ($K_d = 0.35 \cdot H + 0.35$) ($P < 0.001$, $r = 0.90$) and in the combined C57BL/6–Pa groups ($K_d = 0.2 \cdot H - 2.11$) ($P < 0.001$, $r = 0.91$). However, both the slopes and intercepts of the regression lines were different ($P < 0.001$ and

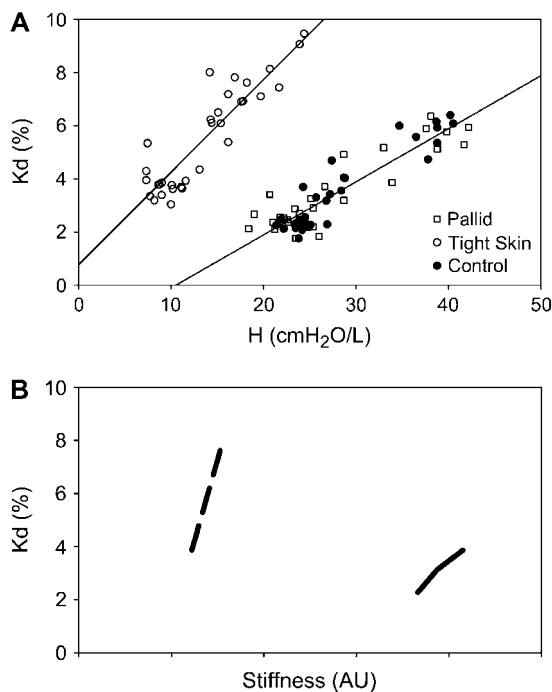


Figure 3. (A) Correlations between H and K_d . The solid lines show separate linear regressions through the Tsk data and the combined data of Pa and C57BL/6. (B) Stiffness– K_d relation from the network model. Stiffness is in arbitrary units. Solid line is from the network in Figure 6A and dashed line is from the network in Figure 6B.

$P < 0.003$), suggesting a significantly stronger nonlinear behavior in the Tsk lung tissue.

Histopathology

Figure 4 shows representative alveolar structures from each group. Significant enlargement of airspaces was observed in the Tsk lungs compared with the C57BL/6 and the Pa lungs. The mean \pm SD of alveolar diameters of the Tsk, Pa, and C57BL/6 lungs were $52.4 \pm 20.1 \mu\text{m}$, $33.5 \pm 12.9 \mu\text{m}$, and $30.7 \pm 7.3 \mu\text{m}$, respectively. Both the mean ($P < 0.01$) and the variance ($P < 0.00001$) of the diameters were significantly larger in the Tsk than in the other two groups. While the mean alveolar diameters did not differ, the variance of the diameters were different ($P < 0.0001$) between the Pa and C57BL/6 groups. There were no differences among the groups in BAL fluid total and differential cell counts.

MAGP Levels

Example Western blots are shown in Figure 5. Quantitative densitometry showed that the lungs of Tsk mice had 3.5% and 6.3% more MAGP-2 than the lungs of Pa and C57BL/6 mice, respectively ($P < 0.01$). However, the levels of MAGP-1, which is a more widespread molecule, were not different among the groups.

Network Modeling

To mimic the mechanics of the normal lung, the stiffness–nonlinearity (Y – K_d) relation was obtained using biaxial sinusoidal stretching superimposed on static biaxial strains of 20%, 25%, and 30%. To account for the remodeling of the alveolar walls, the springs were weakened and made less nonlinear by reducing the value of the nonlinear coefficient a_2 . Furthermore, to mimic the destruction of the alveolar network, 4% of the line elements were eliminated in four steps. First, 1% of the springs

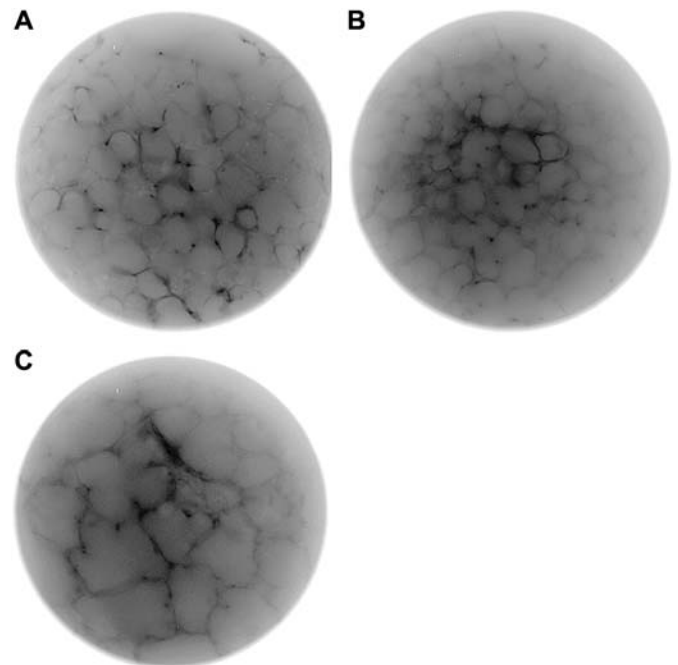


Figure 4. Examples of the auto-fluorescent images of alveolar structures of lung tissues from the C57BL/6 (A), Pa (B), and the Tsk (C) mice.

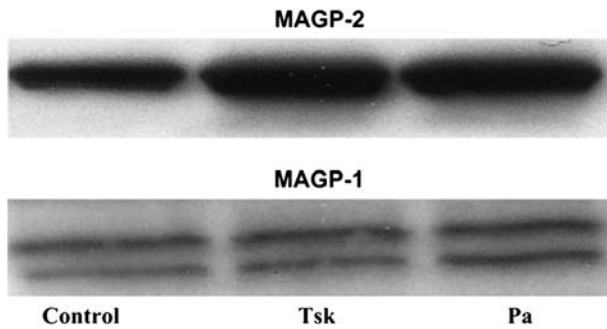


Figure 5. Representative Western blots for Microfibril-Associated Glycoproteins (MAGP) 1 and 2. Note the higher density for MAGP-2 in the Tsk lung.

was randomly eliminated to mimic the random initial breakdown induced by the weakening of the tissue. The network was solved and another 1% of the springs was eliminated this time based on mechanical force: only those elements were cut that carried the largest force. The last step was then repeated two more times, and the $Y-K_d$ relation was calculated corresponding to selected static strain levels as follows. Because the forced oscillatory experiments in the mice were superimposed on static PEEP levels, the initial conditions for these measurements were specified in terms of pressure and not volume. The P–V curves in Figure 1 show that when PEEP was increased from 0 to 3 cm H₂O, lung volume in the Tsk group increased significantly more than that in the Pa group. In the simulations, we mimicked this phenomenon by increasing the static strains from 20%, 25%, and 30% (corresponding to the control lungs) to 30%, 40%, and 50% (corresponding to the Tsk lungs). When the sinusoidal oscillations were superimposed on these static strains, the corresponding $Y-K_d$ relations moved to the left and upward (Figure 3B), suggesting simultaneous weakening of the network and increased nonlinearities in agreement with the data (Figure 3A). The network configurations captured at the peak of the sinusoidal oscillations (Figures 6A and 6B) suggest a significantly increased heterogeneity of the network corresponding to the Tsk simulation: the SD of diameters increased by a factor of 2.6 ($P < 0.03$) similar to that found in the mice. In addition, there are certain springs that carry significantly higher (denoted by red) as well as significantly lower (denoted by blue) forces following the dilution of the network. Indeed, the distribution of forces obtained from four realizations of each condition is much wider and has a longer tail as a consequence of dilution (Figure 6C).

DISCUSSION

The present study aimed at comparing the development of emphysema in the Tsk and the Pa mice. To this end, we assessed the mechanical and dynamic nonlinear properties of the respiratory system, the alveolar structure, and the levels of MAGP 1 and 2. We also used a network model to link elasticity and nonlinearity to tissue destruction and mechanical forces.

Lung Pathophysiology

Both the Tsk and the Pa mice have the same C57BL/6 background. Although emphysema in the Pa mice is linked to lower serum α_1 -antitrypsin concentrations (17), morphologic changes consistent with emphysema were reported to occur only at an age of at least 10 mo (4, 17, 26). It is noteworthy that the Pa mice develop emphysema at an accelerated rate when exposed to cigarette smoke (27). The mean alveolar size and most respira-

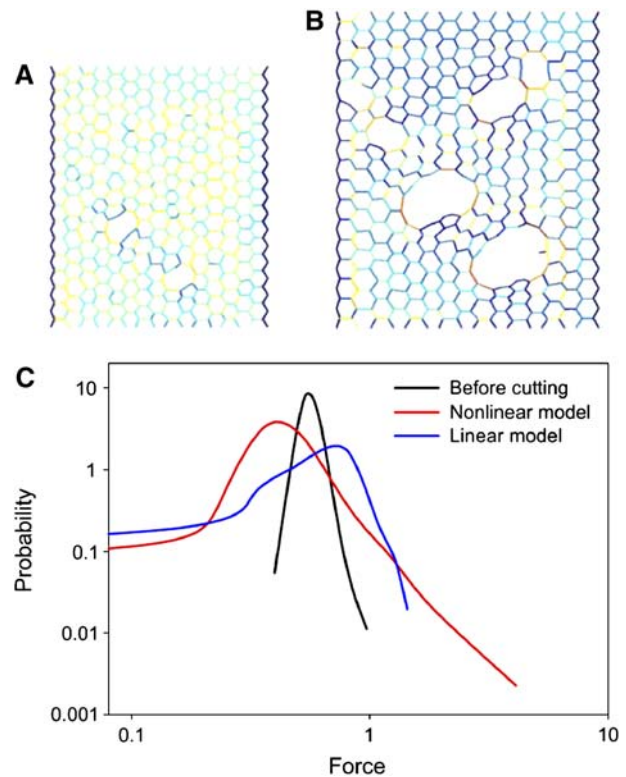


Figure 6. (A) Configuration of the hexagonal network of nonlinearly elastic springs before dilution. (B) Network configuration following the elimination of 4% of the springs and reducing the nonlinear spring constant a_2 . The colors in both A and B are proportional to force on the springs. The different network sizes indicate that they correspond to the same pressure but to different volumes. Note the uniformity of colors in A and the wide distribution of colors in B. (C) Probability density distribution of forces on the line elements from A (black) and B (red). For comparison, the distribution of forces for a linear model is also shown (blue).

tory mechanical parameters of the Pa mice were similar to those of C57BL/6 mice. It is interesting, however, that the MAGP-2 expression in the Pa mice was significantly higher by 3.5% than that in the C57BL/6 mice, which was also accompanied by a more heterogeneous alveolar structure. Thus, while function at the organ level appears nearly normal, there are early signs of subtle abnormalities in the Pa mice at 7 wk of age. The only physiologic parameter that was different between these two groups was Hmax at high PEEP. The significance of this is that because Hmax characterizes the maximum stiffness of the alveolar walls and hence is associated with the properties of collagen, the reduced Hmax in the Pa mice suggests the possibility of early abnormalities in collagen. While these differences are not apparent in the P–V curves or using the single compartment constant phase model of the lung (21), advanced physiologic modeling that accounts for tissue heterogeneity (20) is sensitive to the above noted subtle changes in the periphery of the lung.

Lung elastance including both Hmin and Hmax decreased in all groups with increasing PEEP up to 6 cm H₂O (Figures 2C and 2D) because at low PEEPs, the lungs are partially collapsed in supine mice, which results in high H values. When PEEP increases, H decreases due to recruitment of alveolar regions. The primary functional abnormality in the Tsk was manifested in low H between 0 and 6 cm H₂O of PEEP (Figures 2C and 2D), demonstrating that these lungs expand significantly more

easily than normal lungs. Elastin is known to influence lung elasticity mostly at normal breathing lung volumes (28, 29) corresponding to low PEEPs. The Tsk mice have a decreased elastin content already at an age of 1 mo compared with its control, the Pa mice (30), suggesting that loss of elastin contributes to abnormal tissue elasticity. We also found higher hysteresivity in the Tsk mice than in the Pa and C57BL/6 mice (Figure 2B). Hysteresivity is a macroscopic material property of the tissue (22), which also depends on the microscopic constituents of the alveolar walls. Since changes in the composition and structure of the parenchyma can alter hysteresivity in the emphysematous lung (31–34), our data imply more viscous alveolar walls in the Tsk lung. Another unique observation is the low Raw values in the Tsk group (Figure 2A). While a reduction in Raw ($\sim 20\%$) in emphysema mice has been reported (20, 35), in the present study we found significantly lower values (70%). The decrease in Raw with increasing PEEP is due to the increasing airway diameters with PEEP (Figure 2A). The higher airway diameters in the Tsk mice imply reduced airway wall elasticity.

Since airspace enlargement is documented as early as 4 d of age with progression throughout adult life (5), the Tsk strain is a model of developmental disorder rather than adult-onset emphysema. Tuder and coworkers (36) proposed three potential triggers for emphysema: impaired neonatal septation, architectural defects due to an abnormal microfibrillar lattice, and potential maintenance signaling disruptions due to a loss of matrix sequestration of cytokines. Previously, both airspace enlargement and destruction of elastin were observed in the alveolar walls of the Tsk mice (4, 6, 37). However, the inflammatory component has not been consistently documented (36, 37). We observed no difference in inflammatory cells in the BALF among the groups. In addition, the development of emphysema may not be explained by IL-4, its receptor or TGF- β signaling alone (7, 8). Therefore, the pathophysiology of the Tsk lung reported here may be more related to how fibrillin-1 abnormalities interact with collagen metabolism (1).

Role of Collagen

Abnormal and excessive accumulation of collagen fibers has been reported in various organs of the Tsk mice (38). The skin of these mice is stiffer than normal as assessed from its viscoelastic properties (39). *In vitro* studies also reported increased biosynthesis of collagens including types I, III, and IV by cultured skin and heart fibroblasts (40, 41). Furthermore, significant collagen deposition has been reported in the alveolar septa and increased lung collagen synthesis at 2 mo of age (42). It is therefore unexpected that the lungs of Tsk mice develop emphysema and not fibrosis, and perhaps implies abnormal collagen remodeling. Indeed, collagen turnover is accelerated via degradation by alveolar macrophages (43) that leads to disturbed ultra-structure of collagen in the Tsk mice (6).

An important physiologic consequence of collagen remodeling is the particular PEEP dependence of H (Figures 2C and 2D). Despite its very small values at low PEEPs, H increases beyond a PEEP of 9 cm H₂O in the Tsk mice. Since the stiffening of the lung at higher lung volumes is related to the recruitment of wavy collagen fibers (44), our results suggest that the collagen in the Tsk mice becomes stretched at a lower PEEP than in the Pa mice. In addition, because elastin behaves linearly up to 200% strains (45), the dynamic nonlinearity should also be related to the inherent properties of the collagen fibers (44, 46). Our network modeling clearly demonstrates that following the elimination of walls; some of the remaining walls (and hence the collagen fibers inside them) are significantly more stretched than before the elimination of walls (shown by *red* in Figure 6B). Furthermore, the simulations provide evidence that these overstretched

walls are responsible for the increased dynamic nonlinearities expressed via K_d (Figure 3B) because using linear springs in the network, the K_d became nearly zero. The measured K_d values were linearly related to H in all groups, but the H- K_d relation shifted left and up with an increased slope in the Tsk mice (Figure 3A). Simulations were also able to mimic these features (Figure 3B) suggesting that (1) the decrease in H is partly due to network breakdown (holes in the network) and partly to a decrease in the stiffness of the individual walls (blue regions), (2) the increased K_d is related to the appearance of a few overstretched walls, and (3) the increased slope of the H- K_d relation results from the exaggerated nonlinear behavior of the overstretched walls.

Possible Mechanisms of Progression

The distribution of emphysema lesions is known to be spatially heterogeneous (20, 47, 48). We also found a considerable increase in the variance of alveolar diameters in the Tsk mice ($\sim 400 \mu\text{m}^2$) compared with the Pa ($\sim 170 \mu\text{m}^2$) and C57BL/6 ($\sim 53 \mu\text{m}^2$) mice, which was statistically highly significant ($P < 0.0001$). The existence of such a huge heterogeneity raises the possibility that mechanical forces contribute to the progression of emphysema. If, as a consequence of proteolytic injury, a critical weakening of the ECM takes place in the lung, mechanical forces can accelerate the destruction of the alveolar network (13). When the mechanical stress on a wall reaches a critical value, the wall fails and the stress carried by the wall before failure is redistributed among the neighboring walls, which in turn tend to carry higher than normal stresses and may subsequently fail. Such a progressive destruction governed by mechanical forces necessarily increases the heterogeneity of the structure (13). Mechanical failure has been directly visualized in elastase-treated rats (16), and the failure strength of the alveolar wall in elastase-treated mice is reduced (32). Both of these studies reported an increased SD of alveolar diameters in the emphysematous lungs compared with control. Although the increased SD of alveolar size cannot be interpreted as experimental evidence, it is consistent with the notion that mechanical forces on the alveolar walls due to the distending transpulmonary pressure and the superimposed breathing contribute to disease progression.

The model simulations further support the notion of mechanical stress-induced destruction associated with breathing (*see* animation in the online supplement). While not explored exhaustively, the ability of several other network models, albeit much simpler linear ones, to produce structures compatible with the emphysematous lung has been examined (13). Specifically, it was found that models with random cutting or random cutting with local propagation of defects were not consistent with experimental data (*see* online supplement in Ref. 13). However, force-based cutting does lead to a structure that is in quantitative agreement with the distribution of low attenuation areas on CT images of the lungs from a wide range of patients with emphysema (47). Thus, in this study we further developed the force-based cutting model by including nonlinear mechanisms and predicting the dynamic mechanical and nonlinear properties of the lung. The images in Figure 6 directly visualize the spatial distribution of forces on the walls of this model. Around the perimeter of a larger hole, certain walls carry forces significantly higher than average (*red*), whereas in other directions farther away from the already destroyed regions, the forces can be much less than the average (*blue*). Indeed, the probability distribution of forces in Figure 6C suggests that the elimination of walls significantly widens the distribution. For large forces, the distribution shows a power law tail characterized by a linear decrease on the log-log graph implying a network behavior often seen in complex physiologic systems (49). If the springs in the network

are linear, the distribution for small forces is similar to that in the nonlinear model. However, network breakdown in the linear model only shifts the peak of the distribution to larger forces without generating an extended power law tail. Thus, the network modeling suggests that irregular structure and collagen-related nonlinearities significantly increase mechanical forces on the walls. Consequently, once the failure properties of collagen are compromised, these forces can accelerate the destruction of the parenchyma.

The question is what mechanisms could compromise the failure strength of collagen. Mice lacking fibrillin-1 also develop emphysema via a dysregulation of TGF- β (50), a cytokine that stimulates collagen production. Thus, while the relation between fibrillin-1 abnormality and TGF- β in the Tsk lungs is unclear, it is possible that TGF- β activity is altered, leading to the observed excessive collagen production (42). Perhaps more importantly, MAGP-2 has a direct association with both fibrillin and collagen (18, 19). In response to MAGP-2 stimulation, fibroblast cells in culture increase collagen levels in the ECM without affecting the intracellular mRNA of procollagen. Collagen secreted into the ECM is thermally unstable (51) and in the normal lung only \sim 40% of the secreted molecules are incorporated into existing fibrils (52). However, MAGP-2 is able to stabilize type I collagen (19). An excess of stable collagen in the ECM not only increases collagen levels (42) but may disturb the remodeling process, leading to abnormal collagen assembly. We found that the lungs of Tsk mice had 6.3% and 3.5% more MAGP-2 than the lungs of C57BL/6 and Pa mice, respectively. This suggests that MAGP-2 may be the link between abnormal fibrillin-1 and collagen stabilization and assembly in the Tsk mice. Taken together, these results are consistent with the possibility that abnormalities in collagen fiber assembly and properties combined with mechanical forces play an important role in the development of emphysema in the Tsk mice.

The findings reported here may have implications to human emphysema. First, based on the results in the Pa mice, subtle signs of early emphysema may appear at a much younger age in the α_1 -antitrypsin-deficient patients than previously thought. Second, since interstitial collagenase, which is responsible for the degradation of collagen, is upregulated in human lungs in the late stage of emphysema (53), the results in the Tsk mice raise the possibility that mechanical forces acting on the weakened collagen also contribute to the progressive nature of the human disease.

Conflict of Interest Statement: None of the authors has a financial relationship with a commercial entity that has an interest in the subject of this manuscript.

References

- Kielty CM, Raghunath M, Siracusa LD, Sherratt MJ, Peters R, Shuttleworth CA, Jimenez SA. The tight skin mouse: demonstration of mutant fibrillin-1 production and assembly into abnormal microfibrils. *J Cell Biol* 1998;140:1159–1166.
- Siracusa LD, McGrath R, Ma Q, Moskow JJ, Manne J, Christner PJ, Buchberg AM, Jimenez SA. A tandem duplication within the fibrillin 1 gene is associated with the mouse tight skin mutation. *Genome Res* 1996;6:300–313.
- Visconti RP, Barth JL, Keeley FW, Little CD. Codistribution analysis of elastin and related fibrillar proteins in early vertebrate development. *Matrix Biol* 2003;22:109–121.
- Keil M, Lungarella G, Cavarra E, van Even P, Martorana PA. A scanning electron microscopic investigation of genetic emphysema in tight-skin, pallid, and beige mice, three different C57 BL/6J mutants. *Lab Invest* 1996;74:353–362.
- Martorana PA, van Even P, Gardi C, Lungarella G. A 16-month study of the development of genetic emphysema in tight-skin mice. *Am Rev Respir Dis* 1989;139:226–232.
- O'Donnell MD, O'Connor CM, FitzGerald MX, Lungarella G, Cavarra E, Martorana PA. Ultrastructure of lung elastin and collagen in mouse models of spontaneous emphysema. *Matrix Biol* 1999;18:357–360.
- Kodera T, McGaha TL, Phelps R, Paul WE, Bona CA. Disrupting the IL-4 gene rescues mice homozygous for the tight-skin mutation from embryonic death and diminishes TGF-beta production by fibroblasts. *Proc Natl Acad Sci USA* 2002;99:3800–3805.
- McGaha T, Saito S, Phelps RG, Gordon R, Noben-Trauth N, Paul WE, Bona C. Lack of skin fibrosis in tight skin (TSK) mice with targeted mutation in the interleukin-4R alpha and transforming growth factor-beta genes. *J Invest Dermatol* 2001;116:136–143.
- Janoff A. Elastases and emphysema: current assessment of the protease-antiprotease hypothesis. *Am Rev Respir Dis* 1985;132:417–433.
- Retamales I, Elliott WM, Meshi B, Coxson HO, Pare PD, Sciruba FC, Rogers RM, Hayashi S, Hogg JC. Amplification of inflammation in emphysema and its association with latent adenoviral infection. *Am J Respir Crit Care Med* 2001;164:469–473.
- Turato G, Zuin R, Miniati M, Baraldo S, Rea F, Beghe B, Monti S, Formichi B, Boschetto P, Harari S, *et al.* Airway inflammation in severe chronic obstructive pulmonary disease: relationship with lung function and radiologic emphysema. *Am J Respir Crit Care Med* 2002;166:105–110.
- Vlahovic G, Russell ML, Mercer RR, Crapo JD. Cellular and connective tissue changes in alveolar septal walls in emphysema. *Am J Respir Crit Care Med* 1999;160:2086–2092.
- Suki B, Lutchen KR, Ingenito EP. On the progressive nature of emphysema: roles of proteases, inflammation, and mechanical forces. *Am J Respir Crit Care Med* 2003;168:516–521.
- Barnes PJ, Hansel TT. Prospects for new drugs for chronic obstructive pulmonary disease. *Lancet* 2004;364:985–996.
- Barnes PJ, Stockley RA. COPD: current therapeutic interventions and future approaches. *Eur Respir J* 2005;25:1084–1106.
- Kononov S, Brewer K, Sakai H, Cavalcante FS, Sabayanagam CR, Ingenito EP, Suki B. Roles of mechanical forces and collagen failure in the development of elastase-induced emphysema. *Am J Respir Crit Care Med* 2001;164:1920–1926.
- Martorana PA, Brand T, Gardi C, van Even P, de Santi MM, Calzoni P, Marcolongo P, Lungarella G. The pallid mouse: a model of genetic alpha 1-antitrypsin deficiency. *Lab Invest* 1993;68:233–241.
- Lemaire R, Farina G, Kissin E, Shipley JM, Bona C, Korn JH, Lafyatis R. Mutant fibrillin 1 from tight skin mice increases extracellular matrix incorporation of microfibril-associated glycoprotein 2 and type I collagen. *Arthritis Rheum* 2004;50:915–926.
- Lemaire R, Korn JH, Shipley JM, Lafyatis R. Increased expression of type I collagen induced by microfibril-associated glycoprotein 2: novel mechanistic insights into the molecular basis of dermal fibrosis in scleroderma. *Arthritis Rheum* 2005;52:1812–1823.
- Ito S, Ingenito EP, Arold SP, Parameswaran H, Tgavalekos NT, Lutchen KR, Suki B. Tissue heterogeneity in the mouse lung: effects of elastase treatment. *J Appl Physiol* 2004;97:204–212.
- Hantos Z, Daroczy B, Suki B, Nagy S, Fredberg JJ. Input impedance and peripheral inhomogeneity of dog lungs. *J Appl Physiol* 1992;72:168–178.
- Fredberg JJ, Stamenovic D. On the imperfect elasticity of lung tissue. *J Appl Physiol* 1989;67:2408–2419.
- Suki B, Hantos Z, Daroczy B, Alkaysi G, Nagy S. Nonlinearity and harmonic distortion of dog lungs measured by low-frequency forced oscillations. *J Appl Physiol* 1991;71:69–75.
- Zhang Q, Suki B, Lutchen KR. Harmonic distortion from nonlinear systems with broadband inputs: applications to lung mechanics. *Ann Biomed Eng* 1995;23:672–681.
- Kirkpatrick S, Gelatt CD, Vecchi MP Jr. Optimization by simulated annealing. *Science* 1983;220:671–680.
- de Santi MM, Martorana PA, Cavarra E, Lungarella G. Pallid mice with genetic emphysema. Neutrophil elastase burden and elastin loss occur without alteration in the bronchoalveolar lavage cell population. *Lab Invest* 1995;73:40–47.
- Takubo Y, Guerassimov A, Ghezzi H, Triantafillopoulos A, Bates JH, Hoidal JR, Cosio MG. Alpha1-antitrypsin determines the pattern of emphysema and function in tobacco smoke-exposed mice: parallels with human disease. *Am J Respir Crit Care Med* 2002;166:1596–1603.
- Mead J, Takishima T, Leith D. Stress distribution in lungs: a model of pulmonary elasticity. *J Appl Physiol* 1970;28:596–608.
- Setnikar I. *Arch Fisiol* 1955;55:349–374. (Origin and significance of the mechanical property of the lung) [Italian].
- Gardi C, Martorana PA, de Santi MM, van Even P, Lungarella G. A biochemical and morphological investigation of the early development

- of genetic emphysema in tight-skin mice. *Exp Mol Pathol* 1989;50:398–410.
31. Brewer KK, Sakai H, Alencar AM, Majumdar A, Arold SP, Lutchen KR, Ingenito EP, Suki B. Lung and alveolar wall elastic and hysteretic behavior in rats: effects of in vivo elastase treatment. *J Appl Physiol* 2003;95:1926–1936.
 32. Ito S, Ingenito EP, Brewer KK, Black LD, Parameswaran H, Lutchen KR, Suki B. Mechanics, nonlinearity, and failure strength of lung tissue in a mouse model of emphysema: possible role of collagen remodeling. *J Appl Physiol* 2005;98:503–511.
 33. Lundblad LK, Thompson-Figueroa J, Leclair T, Sullivan MJ, Poynter ME, Irvin CG, Bates JH. Tumor necrosis factor- α overexpression in lung disease: a single cause behind a complex phenotype. *Am J Respir Crit Care Med* 2005;171:1363–1370.
 34. Pillow JJ, Korfhagen TR, Ikegami M, Sly PD. Overexpression of TGF- α increases lung tissue hysteresivity in transgenic mice. *J Appl Physiol* 2001;91:2730–2734.
 35. Collins RA, Ikegami M, Korfhagen TR, Whitsett JA, Sly PD. In vivo measurements of changes in respiratory mechanics with age in mice deficient in surfactant protein D. *Pediatr Res* 2003;53:463–467.
 36. Tuder RM, McGrath S, Neptune E. The pathobiological mechanisms of emphysema models: what do they have in common? *Pulm Pharmacol Ther* 2003;16:67–78.
 37. Rossi GA, Hunninghake GW, Gadek JE, Szapiel SV, Kawanami O, Ferrans VJ, Crystal RG. Hereditary emphysema in the tight-skin mouse: evaluation of pathogenesis. *Am Rev Respir Dis* 1984;129:850–855.
 38. Green MC, Sweet HO, Bunker LE. Tight-skin, a new mutation of the mouse causing excessive growth of connective tissue and skeleton. *Am J Pathol* 1976;82:493–512.
 39. Del Prete Z, Antonucci S, Hoffman AH, Grigg P. Viscoelastic properties of skin in Mov-13 and Tsk mice. *J Biomech* 2004;37:1491–1497.
 40. Bashey RI, Philips N, Insinga F, Jimenez SA. Increased collagen synthesis and increased content of type VI collagen in myocardium of tight skin mice. *Cardiovasc Res* 1993;27:1061–1065.
 41. Jimenez SA, Williams CJ, Myers JC, Bashey RI. Increased collagen biosynthesis and increased expression of type I and type III procollagen genes in tight skin (TSK) mouse fibroblasts. *J Biol Chem* 1986;261:657–662.
 42. Gardi C, Martorana PA, Calzoni P, van Even P, de Santi MM, Cavarra E, Lungarella G. Lung collagen synthesis and deposition in tight-skin mice with genetic emphysema. *Exp Mol Pathol* 1992;56:163–172.
 43. Lucattelli M, Cavarra E, de Santi MM, Tetley TD, Martorana PA, Lungarella G. Collagen phagocytosis by lung alveolar macrophages in animal models of emphysema. *Eur Respir J* 2003;22:728–734.
 44. Suki B, Ito S, Stamenovic D, Lutchen KR, Ingenito EP. Biomechanics of the lung parenchyma: critical roles of collagen and mechanical forces. *J Appl Physiol* 2005;98:1892–1899.
 45. Fung YC. Biomechanics: mechanical properties of living tissues, 2nd ed. New York: Springer-Verlag; 1993.
 46. Maksym GN, Bates JH. A distributed nonlinear model of lung tissue elasticity. *J Appl Physiol* 1997;82:32–41.
 47. Mishima M, Hirai T, Itoh H, Nakano Y, Sakai H, Muro S, Nishimura K, Oku Y, Chin K, Ohi M, et al. Complexity of terminal airspace geometry assessed by lung computed tomography in normal subjects and patients with chronic obstructive pulmonary disease. *Proc Natl Acad Sci USA* 1999;96:8829–8834.
 48. Russi EW, Bloch KE, Weder W. Functional and morphological heterogeneity of emphysema and its implication for selection of patients for lung volume reduction surgery. *Eur Respir J* 1999;14:230–236.
 49. Suki B. Fluctuations and power laws in pulmonary physiology. *Am J Respir Crit Care Med* 2002;166:133–137.
 50. Neptune ER, Frischmeyer PA, Arking DE, Myers L, Bunton TE, Gayraud B, Ramirez F, Sakai LY, Dietz HC. Dysregulation of TGF- β activation contributes to pathogenesis in Marfan syndrome. *Nat Genet* 2003;33:407–411.
 51. Leikina E, Merts MV, Kuznetsova N, Leikin S. Type I collagen is thermally unstable at body temperature. *Proc Natl Acad Sci USA* 2002;99:1314–1318.
 52. McAnulty RJ, Laurent GJ. Collagen synthesis and degradation in vivo: evidence for rapid rates of collagen turnover with extensive degradation of newly synthesized collagen in tissues of the adult rat. *Coll Relat Res* 1987;7:93–104.
 53. Imai K, Dalal SS, Chen ES, Downey R, Schulman LL, Ginsburg M, D'Armiento J. Human collagenase (matrix metalloproteinase-1) expression in the lungs of patients with emphysema. *Am J Respir Crit Care Med* 2001;163:786–791.